Carrier-Induced Silicon Bragg Grating Filters With a p-i-n Junction

Qing Fang, Jun Feng Song, Xiaoguang Tu, Lianxi Jia, Xianshu Luo, Mingbin Yu, and Guo Qiang Lo

***Abstract*— In this letter, we present a carrier-induced silicon waveguide Bragg grating filter with a p-i-n junction. The carrier-induced Bragg grating is formed on the rib silicon waveguide by ion implantation technology. The bandwidth and the extinction ratio of the filter are 0.3 nm and 14 dB, respectively. It can be tuned by both forward and reverse biases. The central wavelength shifting rates under forward and reverse biases are 1.35 and 0.52 pm/V, respectively. The extinction ratio can also be tuned. At the forward bias of 1.5 V, the extinction ratio is reduced from 14 to 5 dB.**

***Index Terms*— Bragg grating filter, carrier-induced, ion implantation, p-i-n junction, silicon photonics.**

I. Introduction

THE BRAGG grating is well known as a crucial filter in optical communications systems, which can be used in various optical devices including optical reflectors, distributed feedback lasers, beam couplers, dispersion compensators, switches, sensors and demultiplexers [1]–[2]. In principle, the pitch of Bragg grating filter is inversely proportional to the effective refractive index of the Bragg grating. In the material systems (such as silica and polymer) with low effective refractive index, the pitch of Bragg grating is quite large and it is easy to fabricate. Up to now, most of Bragg grating research work has been carried out in the silica and polymer materials [3]–[5]. Different technologies have been developed to form the Bragg grating, including dry/wet etching, laser direct-writing and nanoimprint technique. The fabrication of Bragg gratings in high-refractive-index materials such as silicon has a higher challenge due to the small grating pitch. However, silicon-based Bragg grating has been progressively developed recently because silicon photonics have many advantages including compact device sizes, low cost, high volume manufacturability and its compatibility with complementary metal oxide semiconductor (CMOS) technology. A cladding-modulated Bragg grating using periodic placements of cylinders along the channel silicon waveguide was reported [6]. In order to tune the grating by thermo-optic effect, a heater was fabricated on the top of silicon waveguide grating which was formed by dry etching process and the reflected wavelength was shifted to the longer wavelength for the applied voltage [7]–[8]. In the Bragg grating filters formed by the above fabrication technologies, the Bragg grating is permanent once it is formed. Under the thermo-optic or electro-optic modulation, the reflected wavelength of the Bragg grating filter is shifted and the extinction ratio (ER) is hard to change. Recently, an implanted Bragg grating formed on the top of Si waveguide was reported [9]. This grating has a good extinction ratio. However, it is only a passive filter formed using one kind of ion implantation and cannot be tuned. In this letter, we present the first demonstration of a carrier-induced Bragg grating with a p-i-n junction on the rib silicon waveguide by ion implantation technology. The bandwidth and the ER of the grating filter are 0.3 nm and 14 dB, respectively. With the carrier injection, the ER reduces to 5 dB. The central wavelength shifting rates under forward and reverse biases are -1.35 nm/V and 0.52 pm/V, respectively. This kind of carrier-induced Bragg grating shifts the reflected wavelength under the bias and reduces the extinction ratio as well. It can be used potentially as a special tunable filter or switch in wavelength-division multiplexed (WDM) systems, which can guide all waves as a waveguide using a bias and filter a special wave without any bias.

Manuscript received December 26, 2012; revised March 3, 2013; accepted March 5, 2013. Date of publication March 18, 2013; date of current version April 9, 2013. This work was supported in part by the National Natural Science Foundation of China under Grant 61177064 and Singapore A*STAR SERC under Grant 1122804038.

Q. Fang, X. Tu, L. Jia, X. Luo, M. Yu, and G. Q. Lo are with the Institute of Microelectronics, Agency for Science, Technology and Research, 117685 Singapore, and also with the Optoelectronic System Laboratory, Institute of Semiconductor, Chinese Academy of Sciences, Beijing 100083, China (e-mail: fangq@ime.a-star.edu.sg; tux@ime.a-star.edu.sg; jialx@ime.a-star.edu.sg; luox@ime.a-star.edu.sg; mingbin@ime.a-star.edu.sg; logq@ime.a-star.edu.sg).

J. F. Song is with the Institute of Microelectronics, Agency for Science, Technology and Research, 117685, Singapore, and also with the College of Electronic Science and Engineering, Jilin University, Jilin 100015, China (e-mail: Songjf@ime.a-star.edu.sg).

Color versions of one or more of the figures in this letter are available online at http://ieeexplore.ieee.org.

Digital Object Identifier 10.1109/LPT.2013.2252611

II. Design and Fabrication

Fig. 1 shows the schematic configuration of the carrier-induced Bragg grating filter. The rib width of silicon waveguide is 400 nm and the height of the rib waveguide is 220 nm. The slab height is 110 nm. According to the Bragg equation of $\lambda_0 = 2N_{eff}\Lambda$, the grating period Λ of 310 nm is designed for the operation in optical communications wavelength range, where λ_0 is the reflected wavelength of Bragg grating and N_{eff} is the effective refractive index of Bragg grating. In order to simplify the process and reduce the lithography requirement, the duty cycle is 50:50. So, the gap of the implantation finger is 155 nm wide. This gap size is feasible using our 248 nm deep UV lithography tool. Based on the carrier plasma dispersion effect in silicon, the carrier concentration can effectively change the effective refractive index of silicon waveguide in the implantation area.

1041-1135/$31.00 © 2013 IEEE

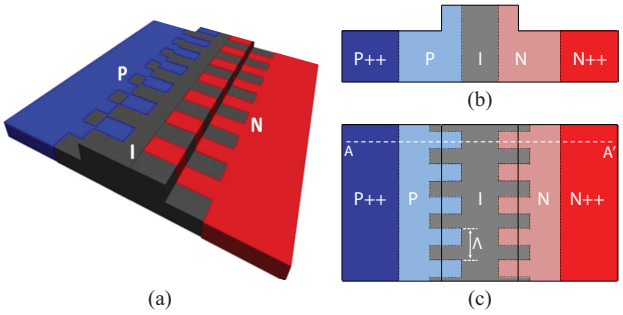

Fig. 1. 3-D structure for the Bragg grating. (a) 3-D structure of Bragg grating with a p-i-n junction. (b) Cross section of the Bragg grating at the AA′ line of (c). (c) Top view of the Bragg grating.

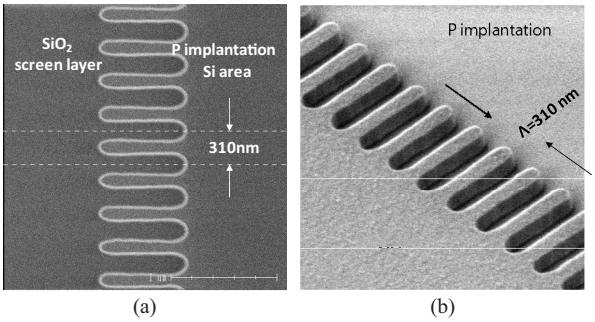

Fig. 2. Scanning electron microscope images of the SiO_2 screen layer for P implantation. (a) Top view. (b) 3-D structure.

We use ion implantation to form the Bragg grating pattern instead of silicon etching process usually used. The implanted modulation width ΔW of the Bragg grating is 150 nm and the length of the Bragg grating is 2000 μm. This kind of Bragg grating filter is based on carrier concentration. Once the carriers move out of the silicon waveguide, this device has not the filter function any more. When the injection carrier concentration is high enough under a forward bias, the Bragg grating profile will be changed and the extinction ratio can also be reduced.

The carrier-induced Bragg grating was fabricated on an 8-inch silicon-on-insulator (SOI) wafer with a 220 nm top Si layer and 2 μm buried oxide. The photo-resist (PR) with high resolution usually has a thin thickness which is not enough to be used as the implantation screen mask. In our experiment, a 1500 Å-thick SiO_2 layer was deposited as the P-type implantation screen layer. After the lithographic process of P-type implantation pattern with the left grating fingers shown in Fig. 1(c), the 1500 Å-thick screen SiO_2 was partially etch by dry etching technology and a 100 Å-thick SiO_2 was remained, as shown in Fig. 2. This remained SiO_2 layer was designed to avoid silicon loss during dry etching process and to avoid silicon surface damage. It is very necessary and critical to the carrier-induced Bragg grating. Then, the boron ion of the dose of $2\times10^{13}/cm^2$ was implanted under the energy of 25 KeV. Another SiO_2 layer of 1500 Å was deposited for the N-type implantation after the first SiO_2 screen layer was completely stripped using the HF solution. Based on the similar processes, the phosphorus ion of the dose of $1\times10^{13}/cm^2$ was implanted under the energy of 80 KeV. After the screen SiO_2 was stripped, the rib waveguide was

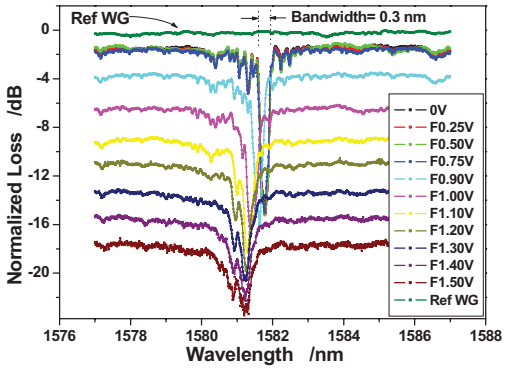

Fig. 3. Optical transmission spectra of the carrier-induced Bragg grating filter with forward biases. The extinction ratio is reduced to 5 dB with +1.5 V bias.

formed by partially etching 110 nm Si. Then, separate masks were used to implant boron and phosphorus into the silicon slab regions to form P++ Ohmic contact and N++ Ohmic contact. The implants were activated via an annealing process at 1030 ^oC for 5 seconds. Finally, the contact vias and the aluminum interconnects was completed.

Agilent optical measurement system (Photonic Dispersion and Loss Analyzer) is used to characterize the optical performances of the carrier-induced silicon Bragg grating filter. The optical measurements are performed after selecting the transverse electric (TE) polarization. First, the similar reference rib silicon waveguide is evaluated. Compared to other carrier-induced Bragg gratings, this reference rib silicon waveguide does not have any implantation. It was fabricated with the carrier-induced Bragg gratings on the same wafer. The measured propagation loss of the rib silicon waveguide is around 1.0 dB/cm at L band for TE mode. After deducting the coupling loss, the normalized transmission spectrum of the reference waveguide is shown in Figs. 3 and 4. The reflected wavelength of Bragg grating is not found in the transmission spectrum of the reference waveguide. Then, the carrier-induced silicon waveguide Bragg grating filter was measured under different forward biases and reverse biases. The transmission spectra under the forward biases are shown in Fig. 3 and the transmission spectra under the reverse biases are shown in Fig. 4. Without any bias applied, there is a reflected wavelength in the transmission spectrum of carrier-induced Bragg grating filter. Compared to the transmission spectrum of the reference waveguide, it proves that the reflected peak results from the ion implantation. The excess optical loss resulted from ion implantation in the Bragg grating filter is about 1.5 dB. So, the optical excess propagation loss caused by ion implantation is about 7.5 dB/cm. The reflected central wavelength is 1581.80 nm. According to the Bragg grating equation, the effective refractive index of this carrier-induced Bragg grating of 2.5513 is calculated. The measured bandwidth is 0.3 nm. Because the effective refractive index change resulted from ion implantation is small, the bandwidth of the carrier-induced Bragg grating is narrow.

With increasing the forward bias, the reflected central wavelength is shifted to the short wavelength side. This shift matches the fact that the forward current increases for the applied voltage shown in the inset of Fig. 5. According to

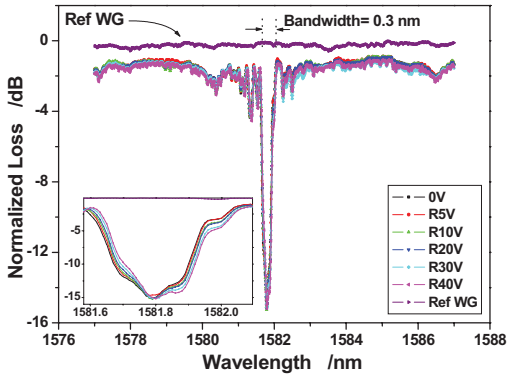

Fig. 4. Optical transmission spectra of the carrier-induced Bragg grating filter with reverse biases (inset: partial enlarged view of the reflected peak).

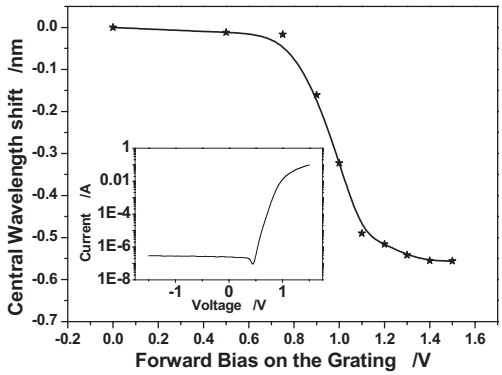

Fig. 5. Reflected central wavelength shifts under forward biases (inset: IV curve of the carrier-induced Bragg grating).

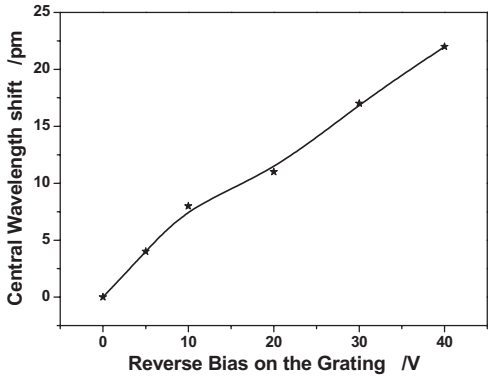

Fig. 6. Reflected central wavelength shifts under reverse biases.

the carrier plasma dispersion effect, the effective refractive index of the waveguide reduces when the carrier concentration increases. Fig. 5 shows the central wavelength shift under the different forward biases in details. From 0.6 V to 1.1 V, the electro-optic effect dominates the wavelength shift and the central wavelength shifting rates is -1.35 nm/V. When the forward voltage is above 1.1 V, the current is quite large and the thermo-optic effect also affects the wavelength shift. Thermo-optic effect raises the effective refractive index and the corresponding wavelength moves to the long wavelength side [7], [10]. So, the peak wavelength of the carrier-induced Bragg grating shifts slower at the higher forward voltage. With the forward current increases, the optical loss increases and the extinction ratio reduces. The increase of the forward current gradually reduces the refractive index difference between the implantation region and the intrinsic region of the carrier-induced Bragg grating. The extinction ratio is only 5 dB at the forward voltage of 1.5 V. Fig. 4 shows the spectra of Bragg grating filter under the reverse biases. Fig. 6 shows is the corresponding wavelength shift results. The wavelength shift rate is ~ 0.52 pm/V. Under the reverse biases, some carriers are swept out from the grating and the grating refractive index slightly increases. So, the reflected central wavelengths shift to the long wavelength side. However, the extinction ratio is hard to change and the wavelength shift rate is small. These results verify that it is hard to sweep out all of the carriers from this kind of p-i-n grating under the reverse bias. The tuning speed of p-i-n devices is faster than the speed of thermal tunable devices. We had reported the tuning speed of a p-i-n device with carrier injection before, which was in the nanosecond range [11].

III. Conclusion

In conclusion, a carrier-induced silicon waveguide Bragg grating with a p-i-n junction has been successfully demonstrated by ion implantation technology for the first time to our knowledge. The bandwidth and the extinction ratio of the grating filter are 0.3 nm and 14 dB, respectively. The reflected central wavelength can be tuned by the bias. The central wavelength shifting rates under forward and reverse biases are -1.35 nm/V and 0.52 pm/V, respectively. With the forward bias of 1.5 V, the extinction ratio reduces to ~ 5 dB.

References

[1] J. Brouckaert, W. Bogaerts, S. Selvaraja, P. Dumon, R. Baets, and D. V. Thourhout, "Planar concave grating demultiplexer with high reflective Bragg reflector facets," *IEEE Photon. Technol. Lett.*, vol. 20, no. 4, pp. 309–311, Feb. 15, 2008.

[2] R. M. Parker, J. C. Gates, M. C. Grossel, and P. G. R. Smith, "In vacuo measurement of the sensitivity limit of planar Bragg grating sensors for monolayer detection," *Appl. Phys. Lett.*, vol. 95, no. 17, pp. 173306-1–173306-3, 2009.

[3] K. Kintaka, J. Nishii, H. Nishiyama, Y. Kawamoto, and A. Sakamoto, "Athermalization of a silica-based waveguide with a UV-induced Bragg grating on a crystallized glass substrate," *J. Lightw. Technol.*, vol. 21, no. 3, pp. 831–836, Mar. 2003.

[4] W. Liang, Y. Huang, Y. Xu, R. K. Lee, and A. Yariv, "Highly sensitive fiber Bragg grating refractive index sensors," *Appl. Phys. Lett.*, vol. 86, no. 15, pp. 151122-1–151122-3, 2005.

[5] A. Kocabas and A. Aydinli, "Polymeric waveguide Bragg grating filter using soft lighography," *Opt. Express*, vol. 14, no. 22, pp. 10228–10232, 2006.

[6] D. T. H. Tan, K. Ikeda, and Y. Fainman, "Cladding-modulated Bragg grating in silicon waveguides," *Opt. Lett.*, vol. 34, no. 9, pp. 1357–1359, 2006.

[7] S. Honda, *et al.*, "Largely-tunable wideband Bragg gratings fabricated on SOI rib waveguides employed by deep-RIE," *Electron. Lett.*, vol. 43, no. 11, pp. 630–631, 2007.

[8] I. Giunton, A. Gajda, M. Krause, R. Steingruber, J. Bruns, and K. Petermann, "Tunable Bragg reflectors on silicon-on-insulator rib waveguides," *Opt. Express*, vol. 17, no. 21, pp. 18518–18524, 2009.

[9] R. Loiacono, *et al.*, "Very low energy implanted Bragg gratings in SOI for wafer scale testing applications," in *Proc. 8th IEEE Int. Conf. Group IV Photon.*, Sep. 2011, pp. 51–53.

[10] Q. Fang, *et al.*, "High efficiency ring-resonator filter with NiSi heater," *IEEE Photon. Technol. Lett.*, vol. 24, no. 5, pp. 350–352, Mar. 1, 2012.

[11] X. Luo, *et al.*, "Silicon high-order coupled-microring-based electro-optical switches for on-chip optical interconnects," *IEEE Photon. Technol. Lett.*, vol. 24, no. 10, pp. 821–823, May 15, 2012.